

gr-qc/9708036
BUTP-97/23
August 17, 1997

Non-Abelian black holes: The inside story ¹

Peter Breitenlohner [§], George Lavrelashvili [‡] ²
and Dieter Maison [§]

Max-Planck-Institut für Physik [§]
— Werner Heisenberg Institut —
Föhringer Ring 6
80805 Munich (Fed. Rep. Germany)

Institute for Theoretical Physics [‡]
University of Bern
Sidlerstrasse 5
CH-3012 Bern, Switzerland

Abstract

Recent progress in understanding of the internal structure of non-Abelian black holes is discussed.

¹Talk given at the international Workshop on The Internal Structure of Black Holes and Spacetime Singularities, Haifa, Israel, June 29 – July 3, 1997

²On leave of absence from Tbilisi Mathematical Institute, 380093 Tbilisi, Georgia

1 Introduction

Let us start recalling what is known about the non-Abelian black holes in general. The non-Abelian story begun in 1988 when Bartnik and McKinnon (BK) unexpectedly found [1] numerically a discrete sequence of globally regular, particle like solutions of the Einstein–Yang–Mills (EYM) theory. Soon the same model was solved with the different boundary conditions corresponding to black holes [2]. Numerical findings were confirmed by mathematically rigorous existence proofs [3, 4] of both regular and black hole solutions. It turned out that all the above solutions of the EYM theory are classically unstable against small perturbations. In addition to the genuine gravitational instabilities [5] there also instabilities of topological origin [6, 7] related to the sphaleron nature of the solitons [8, 9].

A few related systems were investigated. It was shown [10, 11] that the gravitational field can be replaced by a dilaton, so that the YM-dilaton theory in flat space has a tower of solutions similar to the BK sequence. The combined EYMD theory [12, 13, 14, 15, 16] was shown to possess both regular and black hole solutions for any value of the dilaton coupling constant. For the EYMH theory with a Higgs doublet [17] it was shown that the theory in addition to the gravitating sphaleron solution contains its BK type excitations.

Furthermore the EYMH theory with a triplet Higgs [18, 19] was studied. This theory is interesting since in the flat limit it contains t’Hooft-Polyakov monopoles, which are known to be stable. It was shown that the basic monopoles continue to exist, when gravity is switched on, at least as long as the gravitational self-interaction is not too strong. In addition the monopole admits unstable BK type excitations.

Adding a cosmological constant to the EYM theory one obtains non-asymptotically flat analogues of the BK solutions [20, 21].

Whereas in the above study the globally regular solutions were completely analyzed, the investigation of the black hole solutions was not complete since their internal structure was unknown. Recently this problem was investigated independently by us [23] and by Donets, Gal’tsov and Zotov [22]. Our main results on the EYM case essentially agree with theirs, although we differ in some details.

We found it adequate to describe the generic behavior as a kind of mass inflation closely related to the “usual” mass inflation (see e.g. [24, 25, 26, 27,

28] and many references in the present proceedings).

In addition to the generic behaviour there are three different types of special solutions, which are obtained by fine tuning of the initial data at the horizon. There are solutions with Reissner-Nordström (RN), Schwarzschild and pseudo-RN type behaviour.

The present contribution is essentially based on our paper [23].

2 Field Equations

The action of the EYMH theory is

$$S = \frac{1}{4\pi} \int \left(-\frac{1}{4G} R - \frac{1}{4g^2} F^2 + \frac{1}{2} |D_\mu \Phi|^2 - V(\Phi) \right) \sqrt{-g} d^4x, \quad (1)$$

where g denote the gauge coupling constant, G is Newton's constant, F is the field strength of the $SU(2)$ Yang-Mills field and $V(\Phi)$ is the usual quartic Higgs potential. The pure EYM action and corresponding equations can be trivially obtained from the EYMH ones by putting the Higgs field Φ and its potential $V(\Phi)$ to zero.

For the static, spherically symmetric metric we use the parametrization

$$ds^2 = A^2 B dt^2 - \frac{dR^2}{B} - r^2(R) d\Omega^2, \quad (2)$$

with $d\Omega^2 = d\theta^2 + \sin^2 \theta d\varphi^2$ and three independent functions A , B , r of a radial coordinate R , which has, in contrast to r , no geometrical significance. As long as $dr/dR \neq 0$ the simplest choice for r is $R = r$, i.e. Schwarzschild (S) coordinates. In this case it is common to express B through the ‘‘mass function’’ m defined by $B = 1 - 2m/r$.

For the $SU(2)$ Yang-Mills field W_μ^a we use the standard minimal spherically symmetric (purely ‘magnetic’) ansatz

$$W_\mu^a T_a dx^\mu = W(R) (T_1 d\theta + T_2 \sin \theta d\varphi) + T_3 \cos \theta d\varphi, \quad (3)$$

and for the Higgs (triplet) field we assume the form

$$\Phi^a T_a = H(R) n^a T_a, \quad (4)$$

where T_a denote the generators of $SU(2)$ in the adjoint representation. One might also consider other representations for the Higgs, e.g. doublet, but we

believe that the behaviour near $r = 0$ is the same. Plugging these ansätze into the EYM action results in

$$S = - \int dRA \left[\frac{1}{2} \left(1 + B((r')^2 + \frac{(A^2 B)'}{2A^2 B} (r^2)') \right) - Br^2 V_1 - V_2 \right], \quad (5)$$

with

$$V_1 = \frac{(W')^2}{r^2} + \frac{1}{2} (H')^2, \quad (6)$$

and

$$V_2 = \frac{(1 - W^2)^2}{2r^2} + \frac{\beta^2 r^2}{8} (H^2 - \alpha^2)^2 + W^2 H^2. \quad (7)$$

Through a suitable rescaling we have achieved that the action depends only on the dimensionless parameters α and β representing the mass ratios $\alpha = M_W \sqrt{G}/g = M_W/gM_{\text{Pl}}$ and $\beta = M_H/M_W$ (M_H and M_W denoting the Higgs resp. gauge boson mass).

Using S coordinates the field equations obtained from (5) are

$$(BW')' = W \left(\frac{W^2 - 1}{r^2} + H^2 \right) - 2rBW'V_1, \quad (8a)$$

$$(r^2BH')' = (2W^2 + \frac{\beta^2 r^2}{2} (H^2 - \alpha^2))H - 2r^3BH'V_1, \quad (8b)$$

$$(rB)' = 1 - 2r^2BV_1 - 2V_2, \quad (8c)$$

$$A' = 2rV_1A. \quad (8d)$$

If $dr/dR = 0$ (equator!) S coordinates become singular and one has to use a different choice (gauge) for R . A convenient possibility is given by $B \equiv r^{-2}$ for $B > 0$ resp. $B \equiv -r^{-2}$ for $B < 0$. We denote this radial coordinate by τ in order to distinguish it from the S coordinate r . With this choice the metric takes the form

$$ds^2 = - \frac{A(\tau)}{r^2(\tau)} dt^2 + r^2(\tau) (d\tau^2 - d\Omega^2). \quad (9)$$

We will refer to this system of coordinates as isotropic coordinates. The equations obtained with isotropic coordinates are given in [23].

3 Singular points

Obviously the field Eqs. (8) are singular at $r = 0$, $r = \infty$ and for points where B vanishes. Note that a generic solution should have five free parameters for the EYMH case resp. three for the EYM case. Here we have ignored the variable A , which decouples (compare Eq. (8d)).

At the singular points the generic solution is singular and only a non-generic subset of solutions stays regular.

In the vicinity of $r = \infty$ one finds a 3-parameter family of asymptotically flat solutions for the EYMH theory (2-parameter family for the EYM case).

At $r = r_h$ for any given $r_h > 0$ one finds a 3-parameter family characterized by the value of a gauge and Higgs fields at the horizon, W_h and H_h respectively.

In case of the EYM theory it was shown [2, 3, 4] that for any given $r_h > 0$ there is a discrete set of solutions interpolating between the horizon and infinity. They can be characterized by an integer n , the number of nodes of the gauge amplitude W .

The EYMH case is more complicated [18, 19]. Let us here only recall that the previous research was concentrated on the investigation in the interval $[r_h, \infty]$.

Now we turn to the classification of the singular behavior at $r = 0$, which is of particular relevance for the internal structure of black hole solutions. We have to distinguish two cases, $B > 0$ and $B < 0$.

1. $B > 0$: For black holes this case is only possible, if there is a second, inner horizon. One finds a 5-parameter, i.e. generic, family of solutions.

$$W(r) = W_0 + \frac{W_0}{2(1 - W_0^2)} r^2 + W_3 r^3 + O(r^4), \quad (10a)$$

$$H(r) = H_0 + H_1 r + O(r^2), \quad (10b)$$

$$B(r) = \frac{(W_0^2 - 1)^2}{r^2} - \frac{2M_0}{r} + O(1), \quad (10c)$$

where $W_0^2 \neq 1$.

According to the asymptotics of $B(r)$ we may call the singular behavior to be of RN-type. The special case $W_0^2 = 1, M_0 < 0$ leads to S-type behavior with a naked singularity. On the other hand $W_0^2 = 1, H_0 = 0, M_0 = 0$ gives regular solutions.

2. $B < 0$: This case is more involved, with two disjoint families of singular solutions.
- 2.1 There is a 3-parameter family of solutions with a S-type singularity, characterized by the asymptotics

$$W(r) = 1 + W_2 r^2 + O(r^3) , \quad (11a)$$

$$H(r) = H_0 + O(r) , \quad (11b)$$

$$B(r) = -\frac{2M_0}{r} + O(1) . \quad (11c)$$

where $M_0 > 0$.

Obviously the condition $B < 0$ ($M_0 > 0$) prevents the existence of regular solutions in this case.

- 2.2 There is an additional 2-parameter family of solutions with a pseudo-RN singularity (pseudo because $B < 0$).

$$W(r) = W_0 \pm r + O(r^2) , \quad (12a)$$

$$H(r) = H_0 + O(r^2) , \quad (12b)$$

$$B(r) = -\frac{(W_0^2 - 1)^2}{r^2} \pm \frac{4W_0(1 - W_0^2)}{r} + O(1) . \quad (12c)$$

with $W_0^2 \neq 1$. The eigenvalues of the linearized equations are $\lambda_{1,2} = -1/2(3 \pm i\sqrt{15})$ and $\lambda_3 = -1$. This is a repulsive focal point which will turn out to be important for the cyclic behavior in the EYM case.

Note that the corresponding Taylor series for the singular points in case of the EYM theory were listed (with minor mistakes) in [22], whereas in our work [23] the more general EYMH theory was studied and local existence proof was given. In other words we have shown that the expressions above are in fact the beginning of a **convergent** Taylor series for W, H and $r^2 B$.

In the case $B < 0$ we obtained no singular class that has enough parameters (three for EYM and five for EYMH) to describe the generic behavior. Since, also the appearance of a second, inner horizon is a non-generic phenomenon, one may wonder, what the generic behavior inside the horizon near $r = 0$ looks like. This situation is shown schematically on the Fig. 1 for the case of the EYM theory.

4 Numerical results

In order to investigate the generic behavior of non-Abelian black holes inside the event horizon, we integrate the field Eqs. (8)³ from the horizon assuming $B < 0$, ignoring the constraints on the initial data at the horizon required for asymptotic flatness.

Using the Killing time t the horizon is a singular point of the equations. Consequently one has to desingularize the equations in order to be able to start the integration right there. How this can be done, was described in [23, 18].

As one performs the numerical integration one quickly runs into problems due to the occurrence of a quasi-singularity, initiated by a sudden steep raise of W' and subsequent exponential growth of B resp. m (compare Figs. 4, and 5 for some examples). This inflationary behaviour of the mass function is similar to the one observed for perturbations of the Abelian black hole solution at the Cauchy horizon [24, 25, 26, 27]. While this fast growth continues indefinitely for the EYMH system, it comes to a stop without the Higgs field. The mass function reaches a plateau and stays constant for a while until it starts to decrease again. When B has become small enough, i.e. the solution comes close to an inner horizon, the same inflationary process repeats itself. Generically this second “explosion” is so violent (we will give estimates on the increase of m in chapter 5) that the numerical integration procedure breaks down.

Besides these generic solutions there are certain families of special solutions obtained through suitable fine-tuning of the initial data at the horizon. There are two classes of such special solutions. The first class are black holes with a second, inner horizon, the second are solutions with one of the singular behaviours at $r = 0$ for $B < 0$ described in chapter 3. The numerical construction of such solutions is complicated by the fact that both boundary points are singular points of the equations. The strategies employed to solve such problems are well described in the paper on gravitating monopoles [18]. Actually, in order to control the numerical uncertainties we used two different methods, which may be called “matching” and “shooting and aiming”. For matching we integrate independently from both boundary points with

³ At least part of the solutions possess an equator, i.e. a local maximum of r . For those the use of S coordinates is excluded and we integrated the equations in the isotropic coordinates.

regular initial data, tuning these data at both ends until the two branches of the solution match. For shooting and aiming we integrate only from one end and try to suppress the singular part of the solution at the other end by suitably tuning the initial data at the starting point.

Our results concerning special solutions are shown in Fig. 2 and discussed in [23]. As already said, the first class of special solutions consists of black holes with a second, inner horizon; we call them non-Abelian RN-type (NARN) solutions. We have determined two such 1-parameter families for the EYM system, shown in Fig. 2. As may be inferred from Fig. 2, the (dotted) curve 2 corresponding to one such family intersects all (solid) curves describing asymptotically flat solutions except the one for $n = 1$. Curve continues straight through the parabola $r_h = 1 - W_h^2$ and runs all the way to $r_h = W_h = 0$. The branch to the left of the parabola cannot be obtained using S coordinates since solutions develop local maximum of r between the horizons.

Our second NARN family (curve 5 of Fig. 2) stays completely to the left of the parabola and ends at $r_h \approx 0.9$ close to the curve 3, whose significance will be explained below.

The second class are solutions without a second horizon (i.e. B stays negative) approaching the center $r = 0$ with one of the two singular behaviours described in chapter 3, i.e. those with a S-type singularity resp. with a pseudo-RN-type singularity; we denote them NAS resp. NAPRN solutions. We have determined several NAS families represented by the dashed-dotted curves of Fig. 2. The curve 1 staying to the right of the parabola coincides with the corresponding one found in [22], whereas the others, staying essentially to the left of the parabola are new [23]. The basic NAS curve 1 intersects (once) only $n = 1$ (solid) curve for asymptotically flat black holes. As will be explained in chapter 5, the two NAS curves 6 and 7 accompanying the (dotted) NARN curve 5 are expected to merge with the NAS curve 3 close to $r_h = 0.9$. Some of the NAS curves (e.g., 3 and 4) are expected to extend indefinitely to the right, but numerical difficulties (too violent “explosions”) prevented us from continuing them further to larger values of r_h . They will intersect the (solid) curves for asymptotically flat solutions with $n = 2, 3, \dots$ zeros of W and therefore yield additional asymptotically flat NAS black holes.

Asymptotically (for big r_h) the basic NARN curve 2 approaches the basic NAS curve 1. Why this happens can be “understood” from Fig. 3.

Finally there are the NAPRN solutions, which constitute a discrete set

according to the number of available free parameters at $r = 0$. We found several such solutions [23]. Few NAPRN solutions are shown in Fig. 6 and Fig. 7. Only one of them has no maximum of r and was found in [22] as well. Let us stress that although the NAPRN solutions do not correspond to asymptotically flat black holes they play essential role in the explanation on the cyclic behaviour of a generic solution in the EYM case (compare discussion in the next chapter 5).

5 Qualitative Discussion

We shall now give a qualitative picture of the solutions and try to explain our numerical results. Let us briefly summarize what can be done (and what in fact has been done [22, 23])

- get a qualitative understanding of the solutions [22, 23]
- obtain a plateau – to – plateau formula in the EYM case relating quantities at one plateau (before “explosion”) to those on the next plateau (after “explosion”) [23]
- describe a simplified dynamical system, which reflects the main properties of the generic solutions [22, 23]

Since the generic behaviour of the solutions is rather different in the cases with and without Higgs field, we shall treat the two cases separately. Let us first concentrate on the case without Higgs field.

5.1 EYM theory

For a “naive” understanding of the cyclic behaviour one can use a mechanical analogy. Introducing the “time” variable $\sigma = -\ln(r)$ the EYM equations can be written in the form

$$\ddot{W} = \frac{W(W^2 - 1)}{B} - \left[2 + \frac{1}{B} \left(\frac{(W^2 - 1)^2}{r^2} - 1 \right) \right] \dot{W} , \quad (13a)$$

$$\dot{B} = \left(\frac{(W^2 - 1)^2}{r^2} - 1 \right) + \left(1 + \frac{2\dot{W}^2}{r^2} \right) B , \quad (13b)$$

where $\dot{} \equiv d/d\sigma$. The first equation Eq. (13a)) resembles the motion of a fictitious particle in a potential with velocity dependent friction.

Note that the sign of the friction coefficient (term in square brackets in the Eq. (13a)) can be positive as well as negative. Close to the horizon $(W^2 - 1)^2/r^2 - 1 < 0$ and friction coefficient is positive, corresponding to a deceleration of the “particle”. As the time σ increases (r decreases) this term changes sign and the friction turns into anti-friction. The particle starts to accelerate quickly. This leads to a domination of the second term (kinetic energy) in Eq. (13b), which in turn leads to a fast growth of the function B (respectively m). But growth of B stops the anti-friction in Eq. (13a) and the particle is again in the slow roll regime until the next “explosion”.

For more detailed discussion of the generic behaviour we introduce the notation $\bar{U} \equiv BW'$ and $\bar{B} \equiv rB$ and use again $\sigma \equiv -\ln(r)$ as a radial coordinate [23]. Note that $\bar{B} \approx -2m$ for small r . With these variables the field Eqs. (8)

$$\dot{W} = -r^2 \frac{\bar{U}}{\bar{B}}, \quad (14a)$$

$$\dot{\bar{U}} = -W \frac{W^2 - 1}{r} + 2r^2 \frac{\bar{U}^3}{\bar{B}^2}, \quad (14b)$$

$$\dot{\bar{B}} = r \left(\frac{(1 - W^2)^2}{r^2} - 1 \right) + 2r^2 \frac{\bar{U}^2}{\bar{B}}. \quad (14c)$$

Close to the horizon the first term in the equation for \bar{B} dominates (since \bar{U} vanishes at $r = r_h$) and thus \bar{B} becomes negative. Provided W^2 does not tend to 1, this term will, however, change sign as r decreases and \bar{B} will turn back to zero. Assuming further that \bar{U} does not tend to zero simultaneously, the second term in the equation for \bar{U} will grow very rapidly as \bar{B} approaches zero, leading to a rapid increase of \bar{U} . This in turn induces a rapid growth of \bar{B} (compare Fig. 4). Once the second terms in Eqs. (14b,c) dominate one gets $(\bar{U}/\bar{B}) \approx 0$ and thus $\bar{U}/\bar{B} = W'/r$ tends to a constant c . As long as $(rc)^2$ is sizable \bar{U} and \bar{B} increase exponentially, giving rise to the phenomenon of mass inflation. Eventually this growth comes to a stop when $(rc)^2$ has become small enough. Then \bar{U} and \bar{B} stay constant until the first terms in Eqs. (14b,c) become sizable again. As before \bar{B} tends to zero inducing another “explosion” resp. cycle of mass inflation (compare Fig. 4).

In the discussion above we made two provisions – that W^2 stays away from 1 and that \bar{U} does not tend to zero simultaneously with \bar{B} . If the first condition is violated, i.e. $W^2 \rightarrow 1$ we get a NAS solution. If on the

other hand \bar{U} and \bar{B} develop a common zero we get a NARN solution, i.e. a solution with a second horizon. Both these phenomena can occur after any finite number of cycles, giving rise to several NAS resp. NARN curves as in Fig. 2. Generically W changes very little during an inflationary cycle, with the exception of solutions that come very close to a second horizon, i.e. close to a NARN solution. In this case W may change by any amount, depending on how small \bar{U} becomes at the start of the explosion. By suitably fine-tuning the initial data at the horizon one can then obtain new NAS solutions with $W \rightarrow \pm 1$ or a new NARN solution. In this way each NARN solution is the ‘parent’ of two NAS and one NARN solution. This schematically shown on the Fig. 8. Fig. 2 shows two such generations: the NARN solutions labelled 2 have the NAS children 3 and 4 and the NARN child 5; the curves labelled 6 and 7 are the NAS children of 5. Whenever the value of W at the second horizon of a NARN solution approaches ± 1 this NARN curve and its NAS children merge with the corresponding sibling NAS curve having one cycle less. This hierarchy of special solutions gives rise to a kind of chaotic structure in this region of “phase space”.

Neglecting irrelevant terms one can integrate Eqs. (14) and obtain a plateau – to – plateau relation [23], which connects the quantities W_0, \bar{U}_0 and \bar{B}_0 before an explosion with $W_1, \bar{U}_1, \bar{B}_1$ after it ⁴

$$\bar{U}_1 = \bar{U}_0 e^{(cr_0)^2}, \quad \bar{B}_1 = \frac{\bar{U}_0}{c} e^{(cr_0)^2}, \quad W_1 = W_0 - \frac{c}{2} r_0^2, \quad (15)$$

with

$$r_0 = -\frac{(W_0^2 - 1)^2}{\bar{B}_0}, \quad c = \frac{(W_0^2 - 1)^2}{2\bar{U}_0 r_0^3}. \quad (16)$$

It is instructive to illustrate these relations on an example. We take the fundamental black hole solution with $r_h = 1$ and $W_h = 0.6322$ shown in Fig. 1 in [23]. For the first explosion one finds the parameters $r_0 \approx 2.7 \cdot 10^{-4}$ and $c \approx 1.1 \cdot 10^5$ yielding $cr_0 \approx 30$ and thus $\bar{B}_1 \sim e^{900}$ and $W_1 - W_0 \approx 4 \cdot 10^{-3}$. The subsequent explosion will then take place at the fantastically small value $r_0 \sim e^{-900} \approx 10^{-330}$.

Since the change of W in one inflationary cycle has an extra factor r_0 the function W stays practically constant. If we furthermore concentrate on cases, where the first term in Eq. (14b) can be neglected we may use the

⁴Note that the similar relations are obtained recently in [29].

simplified system [22, 23]

$$\dot{W} = 0, \quad \dot{U} = 2r^2 \frac{\bar{U}^3}{\bar{B}^2}, \quad \dot{B} = \frac{(1 - W^2)^2}{r} + 2r^2 \frac{\bar{U}^2}{\bar{B}}. \quad (17)$$

Introducing the variables $x \equiv r\bar{U}/\bar{B} = W'$ and $y \equiv -(1 - W^2)^2/r\bar{B}$ one obtains the autonomous system

$$\dot{W} = 0, \quad \dot{x} = (y - 1)x, \quad \dot{y} = y(y + 1 - 2x^2). \quad (18)$$

Since the first of these equations may be ignored, we can concentrate on the x, y part. As usual for 2-dimensional dynamical systems the global behavior of the solutions can be analyzed determining its fixed points. Since the “large time” behavior $\sigma \rightarrow \infty$ corresponds to the limit $r \rightarrow 0$ these fixed points are related to the singular solutions at $r = 0$ discussed in chapter 3. There are essentially three different fixed points.

1. For $y < 0$ there is the fixed point $x = 0, y = -1$ giving the RN type singularity. Its eigenvalues are -1 and -2 , hence it acts as an attracting center for $\sigma \rightarrow \infty$.
2. Then there is the point $x = y = 0$, a saddle with eigenvalues ± 1 .
3. In addition there are the points $x = \pm 1, y = 1$ with the eigenvalues $1/2(1 \pm i\sqrt{15})$, related to the pseudo-RN type singularity. This fixed point acts as a repulsive focal point, from which the trajectories spiral outwards. Since solutions of the approximate system given by the Eqs. (18) cannot cross the coordinate axes, solutions in the quadrants $y > 0, x > 0$ resp. $x < 0$ stay there performing larger and larger turns around the focal point coming closer and closer to the saddle point $x = y = 0$ without ever meeting it. As observed in [22] this nicely explains the cyclic inflationary behaviour of the solutions in the generic case.

It is interesting to note that the similar results were obtained in the Abelian case [26, 27] in the homogeneous mass inflation model ⁵.

⁵We are thankful to A.Ori for bringing the ref. [26] to our attention and for communicating his unpublished results [27].

5.2 EYMH theory

Finally let us discuss the black holes with Higgs field. Apart from the generic solutions there are the special ones approaching $r = 0$ with a singular behaviour described in chapter 3. On the other hand, the generic behaviour is much simpler than in the previously discussed situation without Higgs field. An easy way to understand this difference is to derive the analogue of the simplified system Eqs. (18). Introducing the additional variable $z \equiv -\dot{H}$ and ignoring again irrelevant terms one finds [23]

$$\dot{W} = 0, \quad \dot{H} = -z, \quad (19a)$$

$$\dot{x} = (y - 1)x, \quad \dot{z} = yz \quad (19b)$$

$$\dot{y} = y(y + 1 - 2x^2 - z^2). \quad (19c)$$

Leaving aside the decoupled equations for W and H one may study the fixed points of the (x, y, z) system. For $z = 0$ one clearly finds the previous fixed points of the (x, y) system. However, for $z \neq 0$ the focal point disappears and the only fixed point for $y \geq 0$ is $x = y = 0, z = z_0$ with some constant z_0 . For $z_0^2 < 1$ this point is a saddle with one unstable mode, whereas for $z_0^2 > 1$ it is a stable attractor. The latter describes the simple inflationary behavior described in chapter 4 and shown in the left part of Fig. 5. Solutions approaching a fixed point with $z_0^2 < 1$ eventually run away from it again and ultimately tend to one with $z_0^2 > 1$ as shown in the right part of Fig. 5.

In the limit the equations can be trivially integrated with the result

$$y = y_0 e^{(1-z_0^2)\sigma} = y_0 r^{z_0^2-1}. \quad (20)$$

Thus the mass function grows exponentially in “time” σ or as a power in terms of r

$$m = m_0 e^{z_0^2 \sigma} = \frac{m_0}{r^{z_0^2}} \quad (21)$$

in perfect agreement with our numerical results Fig. 5. Note that the fixed point Eq. (20) differs from the ones listed in the chapter 3 since the nature (strength) of the singularity depends on the solution itself. This fixed point was “rediscovered” in [30].

Note that the inclusion of a scalar field in the homogeneous mass inflation model [27] has the same effect as the addition of the Higgs field to the EYM theory, namely that the mass inflation cycles disappear.

6 Concluding remarks

To summarize the interior geometry of non-Abelian black holes exhibits a very interesting and complicated structure. Besides the generic solutions there are special NAS, NARN and NAPRN solutions, which can be obtained by a fine tuning initial data at the horizon. The main conclusion is that no inner (Cauchy) horizon is formed inside non-Abelian black holes in generic case, instead one obtains a kind of mass inflation. Without a Higgs field, i.e. for the EYM theory, this mass inflation repeats itself in cycles of ever more violent growth.

A natural question to ask is what might be potential outcome of this investigation. A short answer would be

- illustration of singularity theorems [31]
- possible cosmological applications (see e.g. [30])
- interesting laboratory for non-perturbative study of (homogeneous) mass inflation phenomenon

Naturally one should bare in mind limitations which come from quantum corrections and instability. Our consideration was purely classical, but when r tends to zero the curvature diverges and quantum corrections will become important. As it was discussed in the Introduction the EYM and most of the EYMH black holes are classically unstable. What will be a fate of a non-static perturbations inside non-Abelian black holes is an interesting open question. Definitely these subjects require further study.

7 Acknowledgments

G.L. is grateful to the organizers for the invitation to Haifa and kind hospitality extended during the conference.

The work of G.L. was supported in part by the Tomalla Foundation and by the Swiss National Science Foundation.

References

- [1] R. Bartnik and J. McKinnon, *Particlelike Solutions of the Einstein–Yang–Mills Equations*, *Phys. Rev. Lett.* **61** (1988) 141–144.

- [2] H.P. Künzle and A.K.M. Masood-ul-Alam, *Spherically symmetric static SU(2) Einstein–Yang–Mills fields*, *J. Math. Phys.* **31** (1990) 928–935;
M.S. Volkov and D.V. Gal'tsov, *Non–Abelian Einstein–Yang–Mills black holes*, *JETP Lett.* **50** (1990) 345–350;
P. Bizon, *Colored Black Holes*, *Phys. Rev. Lett.* **61** (1990) 2844–2847.
- [3] J.A. Smoller, A.G. Wasserman, and S.T. Yau, *Existence of black hole solutions for the Einstein / Yang–Mills equations*, *Comm. Math. Phys.* **154** (1993) 377–411;
J.A. Smoller and A.G. Wasserman, *Existence of infinitely many smooth, static, global solutions of the Einstein / Yang–Mills equations*, *Comm. Math. Phys.* **151** (1993) 303–325.
- [4] P. Breitenlohner, P. Forgacs, and D. Maison, *On Static spherically symmetric solutions of the Einstein–Yang–Mills equations*, *Commun. Math. Phys.*, **163** (1994) 141–172.
- [5] N. Straumann and Z.H. Zhou, *Instability of the Bartnik–McKinnon solution of the Einstein–Yang–Mills equations*, *Phys. Lett.* **B237** (1990) 353–356;
Instability of a colored black hole solution, *Phys. Lett.* **B243** (1990) 33–35.
- [6] G. Lavrelashvili and D. Maison, *A Remark on the instability of the Bartnik–McKinnon solutions*, *Phys. Lett.*, **B343** (1995) 214–217.
- [7] M.S. Volkov, O. Brodbeck, G. Lavrelashvili and N. Straumann, *The Number of sphaleron instabilities of the Bartnik–McKinnon solitons and non-Abelian black holes*, *Phys. Lett.* **B349** (1995) 438–442.
- [8] D.V. Gal'tsov and M.S. Volkov, *Sphalerons in Einstein–Yang–Mills theory*, *Phys. Lett.* **B273** (1991) 255–259;
D. Sudarsky and R.M. Wald, *Extrema of mass, stationarity, and staticity, and solutions to the Einstein–Yang–Mills equations*, *Phys. Rev.* **D46** (1992) 1453–1474;
I. Moss and A. Wray, *Black holes and sphalerons*, *Phys. Rev.* **D46** (1992) 1215–1218;
G.W. Gibbons and A.R. Steif, *Yang–Mills cosmologies and collapsing gravitational sphalerons*, *Phys. Lett.* **B320** (1994) 245–252.

- [9] G. Lavrelashvili, *Fermions in the background of dilatonic sphalerons*, *Mod. Phys. Lett.* **A9** (1994) 3731–3740.
- [10] G. Lavrelashvili and D. Maison, *Static spherically symmetric solutions of a Yang–Mills field coupled to a dilaton*, *Phys. Lett.* **B295** (1992) 67–72.
- [11] P. Bizon, *Saddle-point solutions in Yang–Mills–dilaton theory*, *Phys. Rev.* **D47** (1993) 1656–1663.
- [12] G. Lavrelashvili and D. Maison, *Regular and black hole solutions of Einstein–Yang–Mills dilaton theory*, *Nucl. Phys.* **B410** (1993) 407–422;
G. Lavrelashvili, *Black holes and sphalerons in low–energy effective string theory*, hep-th/9410183.
- [13] P. Bizon, *Saddle points of stringy action*, *Acta Physica Polonica* **B24** (1993) 1209–1220.
- [14] E.E. Donets and D.V. Gal'tsov, *Stringy sphalerons and non–abelian black holes*, *Phys. Lett.* **B302** (1993) 411–418.
- [15] T. Torii and Kei-ichi Maeda, *Black holes with non–Abelian hair and their thermodynamical properties*, *Phys. Rev.* **D48** (1993) 1643–1651.
- [16] B. Kleihaus, J. Kunz, and A. Sood, *$SU(3)$ Einstein–Yang–Mills dilaton sphalerons and black holes*, *Phys. Lett.* **B372** (1996) 204–211.
- [17] B.R. Greene, S.D. Mathur, and C.M. O'Neill, *Eluding the no hair conjecture: Black holes in spontaneously broken gauge theories*, *Phys. Rev.* **D47** (1993) 2242–2259.
- [18] P. Breitenlohner, P. Forgacs, and D. Maison,
Gravitating monopole solutions, *Nucl. Phys.*, **B383** (1992) 357–376;
Gravitating monopole solutions. 2, *Nucl. Phys.*, **B442** (1995) 126–156.
- [19] K. Lee, V.P. Nair, and E.J. Weinberg, *Black holes in magnetic monopoles*, *Phys. Rev.* **D45** (1992) 2751–2761.
- [20] T. Torii, Kei-ichi Maeda, and T. Tachizawa, *Cosmic colored black holes*, *Phys. Rev.* **D52** (1995) 4272–4276.

- [21] M.S. Volkov, N. Straumann, G. Lavrelashvili, M. Heusler, and O. Brodbeck, *Cosmological Analogues of the Bartnik–McKinnon Solutions*, *Phys. Rev.*, **D54** (1996) 7243–7251.
- [22] E.E. Donets, D.V. Gal'tsov, M.Yu. Zotov, *Internal Structure of Einstein–Yang–Mills Black Holes*, gr-qc/9612067, versions 1–4.
- [23] P. Breitenlohner, G. Lavrelashvili, and D. Maison, *Mass inflation and chaotic behaviour inside hairy black holes*, gr-qc/9703047.
- [24] E. Poisson and W. Israel, *Internal structure of black holes*, *Phys. Rev.*, **D41** (1990) 1796–1809.
- [25] A.Ori, *Inner Structure of a Charged Black Hole: An Exact Mass–Inflation Solution*, *Phys. Rev. Lett.*, **67** (1991) 789–792;
Structure of the Singularity inside a Realistic Rotating Black Hole, *Phys. Rev. Lett.*, **68** (1992) 2117–2120.
- [26] D.N. Page, *Black–Hole Thermodynamics, Mass–Inflation, and Evaporation*, in: *Black Hole Physics*, V. De Sabbata and Z. Zhang (eds.), (Kluwer, 1992), p. 185–224.
- [27] A.Ori, 1991, (unpublished).
- [28] A. Bonanno, S. Droz, W. Israel, and S.M. Morsink, *Structure of the inner singularity of a spherical black hole*, *Phys. Rev.*, **D50** (1994) 7372–7375.
- [29] D.V. Gal'tsov, E.E. Donets, M.Yu. Zotov, *Singularities inside non–Abelian black holes*, *JETP Lett.* **65** (1997) 855.
- [30] D.V. Gal'tsov, and E.E. Donets, *Power-law mass inflation in Einstein–Yang–Mills–Higgs black holes*, gr-qc/9706067.
- [31] S.W. Hawking, and G.F.R. Ellis, *The large scale structure of space-time*, Cambridge University Press, 1973.

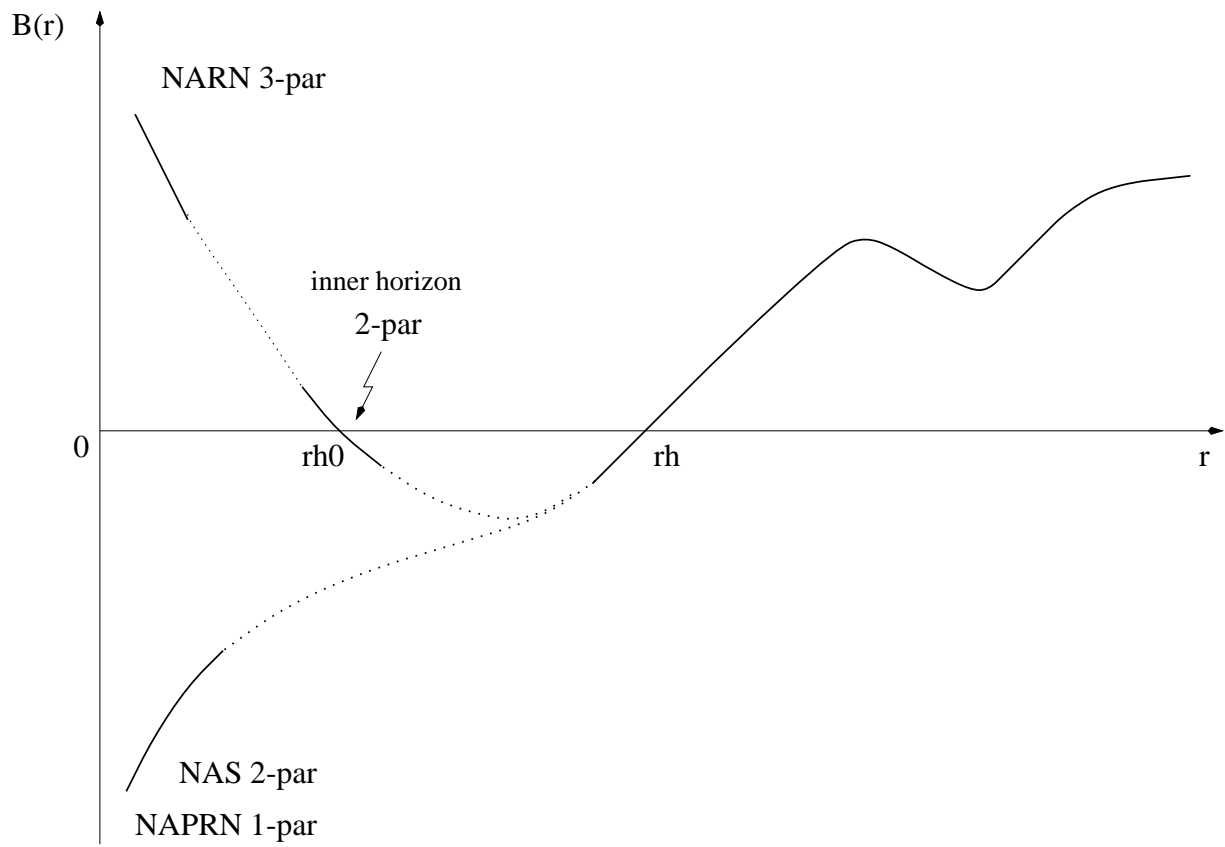


Figure 1: Schematic view of the different special solutions in the EYM theory.

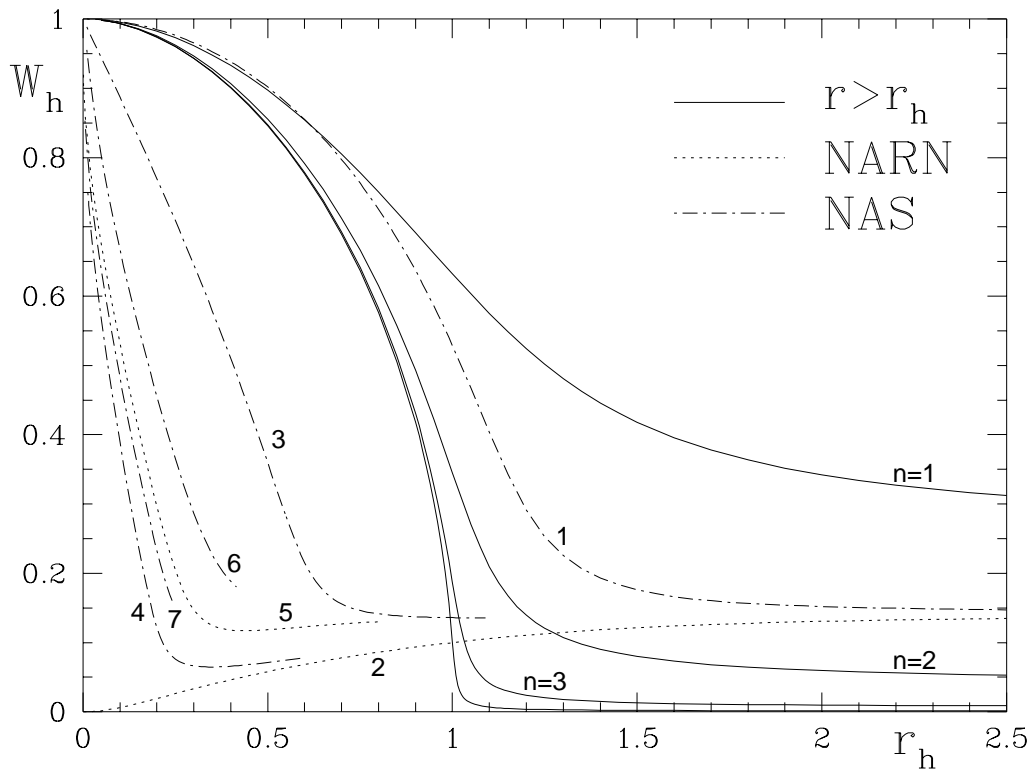


Figure 2: Initial data for special solutions. The solid curves represent asymptotically flat solutions with n zeros of W . The other curves represent various NARN and NAS families.

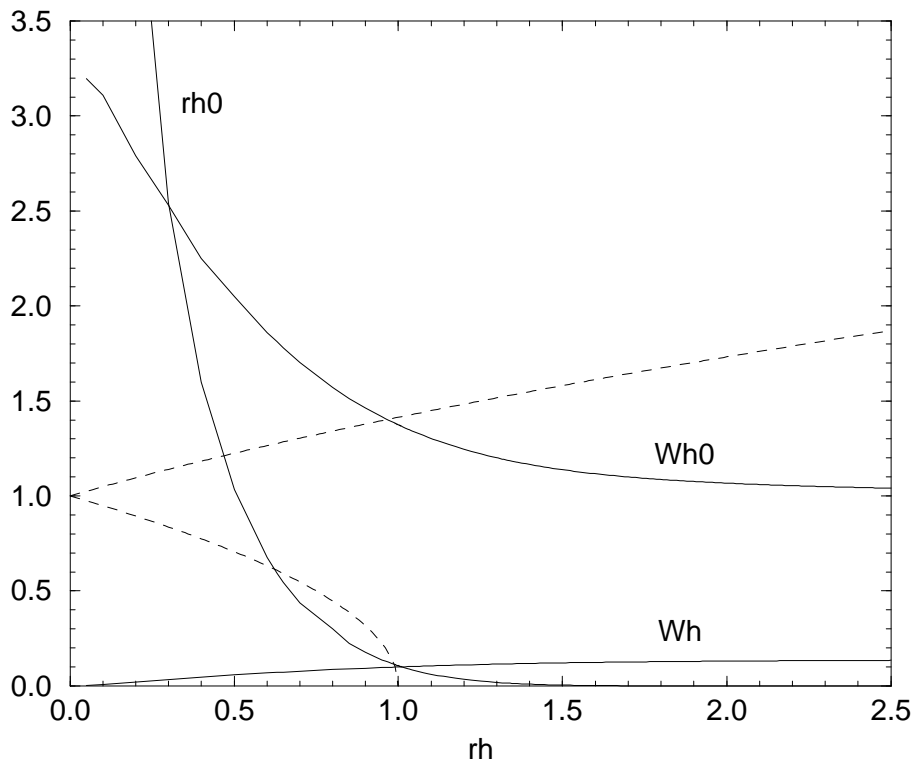


Figure 3: Parameters of the basic (lowest) NARN solutions. One clearly sees that with increasing r_h the value of the second (inner) horizon $r_{h0} \rightarrow 0$ and value of the gauge field there $W_{h0} \rightarrow 1$. This values correspond to NAS solutions.

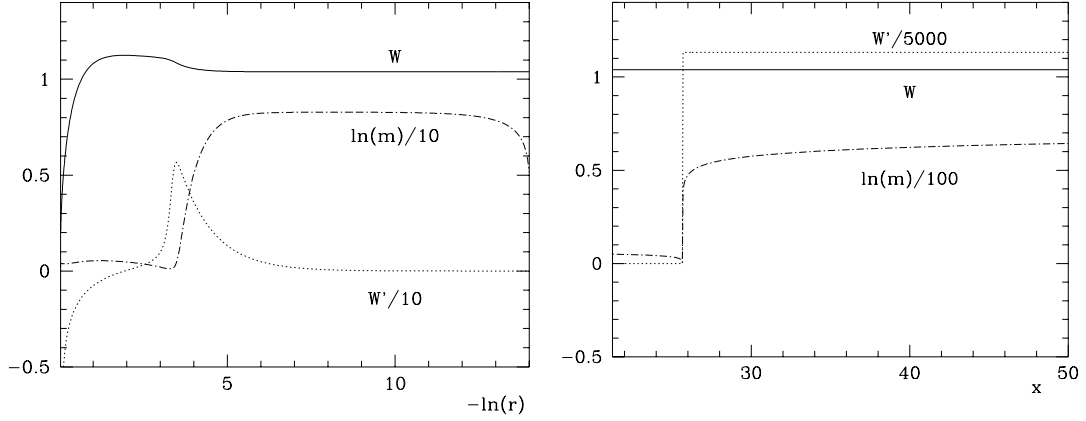


Figure 4: First two cycles of the solution with $r_h=0.97$ and $W_h = 0.2$. For the second cycle a suitably stretched coordinate x is used.

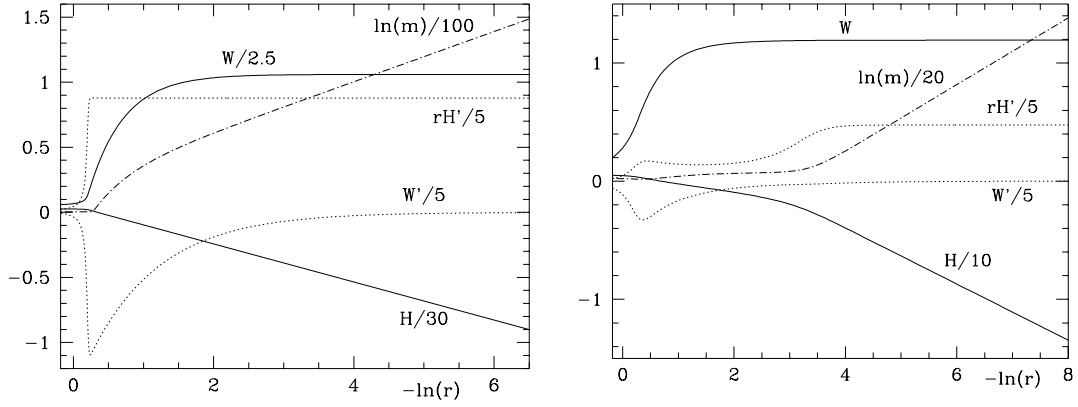


Figure 5: Two characteristic types of inflationary solutions with Higgs fields. Note that in both cases asymptotically $\ln(m)$ is linear in $\ln(r)$.

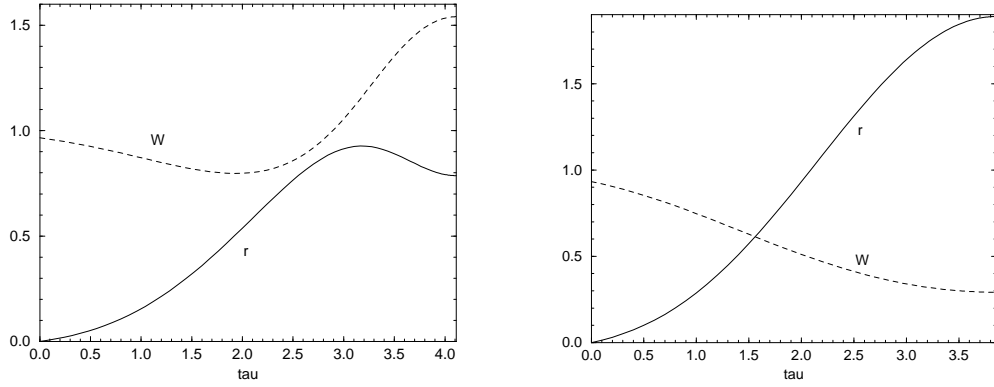


Figure 6: Two different NAPRN solutions with no zero of W between $r = 0$ and $r = r_h$.

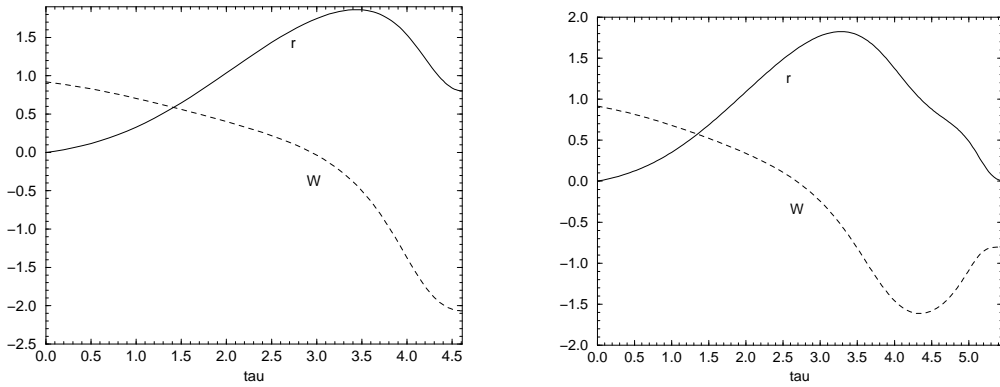


Figure 7: Two different NAPRN solutions with one zero of W between $r = 0$ and $r = r_h$.

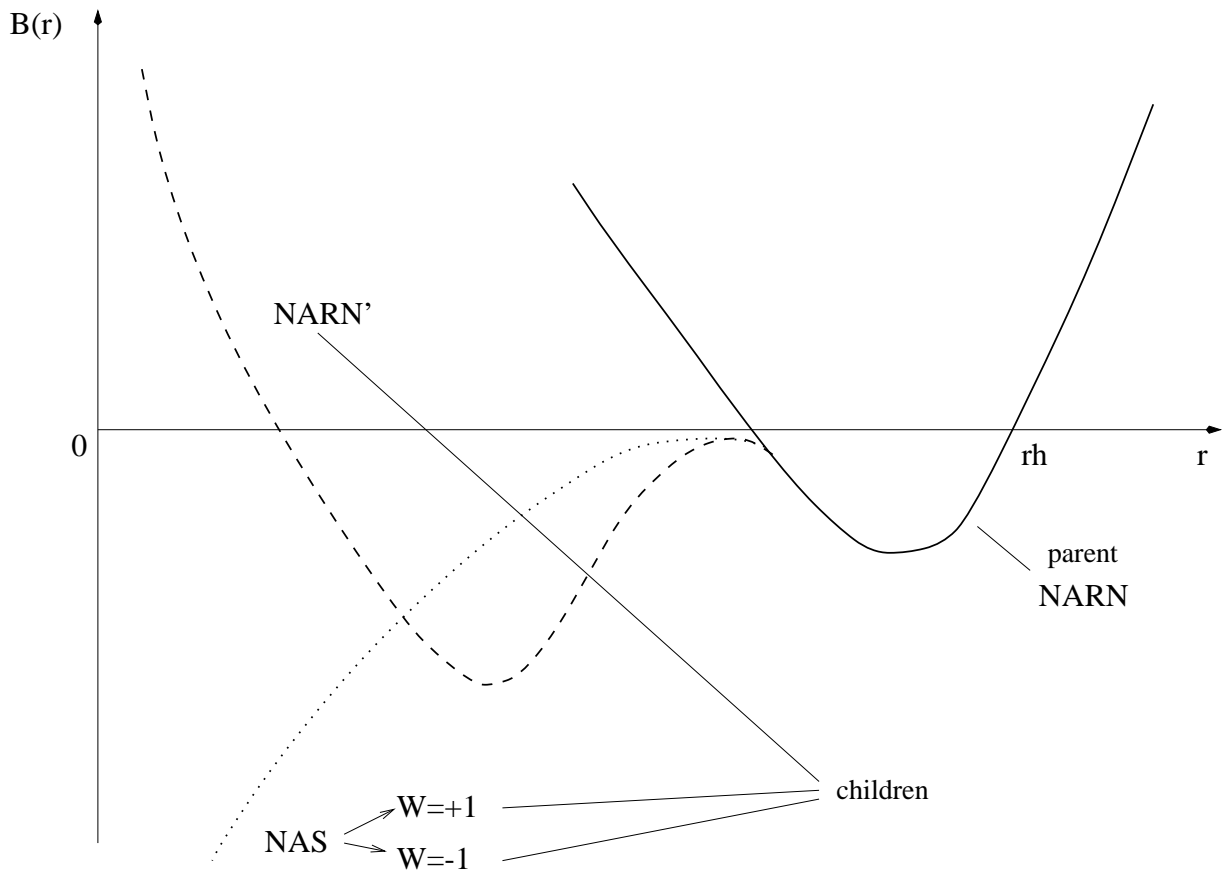


Figure 8: Schematic view of the NARN solutions and their children.